IJRCS

International Journal of Robotics and Control Systems
Vol. 5, No. 1, 2025, pp. 124-138
ISSN 2775-2658
http://pubs2.ascee.org/index.php/ijrcs

ASCEE

Effect of Different Hinge Angles on Control Performance Metrics and Disturbance Rejection in Swashplateless Micro Aerial Robots

Ali Tahir Karasahin [a,1,*]

[a] Department of Mechatronics Engineering, Necmettin Erbakan University, Meram, Konya 42090, Turkey
[1] alitahir.karasahin@erbakan.edu.tr
[*] Corresponding Author

ARTICLE INFO

Article History
Received October, 10 2024
Revised November, 12 2024
Accepted December, 05 2024

Keywords
Aerial Robotics;
Swashplateless Mechanism;
Cyclic Modulation

ABSTRACT

Micro Aerial Robots (MARs) have demonstrated outstanding performance in autonomous applications, making the performance of their controllers critical. The development of controllers for aerial robots using alternative designs rather than standard ones requires that their performance be investigated using different approaches prior to flight. Hence, this paper presents a 2-degree-of-freedom (DOF) test platform designed to evaluate both controller performance and the swashplateless mechanism that generates orientation and position changes. Recent studies have indicated a need to determine the relationship between the hinge angle and controller performance in the context of swashplateless mechanisms. This paper found that the different hinge angles and controller performance relationships on the 2-DOF test platform are investigated through reference tracking and wind disturbance tests. The swashplateless mechanism with a hinge angle of 30° showed better performance in terms of control sensitivity and wind disturbance rejection compared to 45° and 60° hinge angles. Disturbance rejection performance has been tested at a wind speed of 3.3 m/s simulating moderate outdoor wind conditions. The results show that different hinge angles affect controller performance in terms of rise and settling time, overshoot and integral of time absolute of error (ITAE). It has been shown that the choice of hinge angle in the swashplateless mechanism should be such to improve flight performance according to specific application and performance requirements. In addition to advancing the design and control of MARs, these results are expected to contribute to improvements in potential application areas of aerial robots, such as inspection and sensing.

1. Introduction

Micro Aerial Robots (MARs) have had many applications in recent years because they are cost-efficient and reachable. These robots are used in a wide range of applications, such as cooperative transportation, power line inspection and research and rescue operations, learning biomimetic behaviours [1]–[10]. In addition, this system stands out as an aerial robot highly valuable in areas where human operation is difficult or risky. MARs are preferred because of their low power consumption and volume. These systems have a different framework such as quadcopter [11], [12], robotic hummingbird [13], [14] and coaxial-rotor unmanned aerial vehicle (UAV) [15], [16].

Quadcopters are preferred for their basic design, high maneuver capability and acceptable flight time. For these reasons stated this platform has achieved notable success in applications such as agile flight [17]–[20], learning high-speed flight [21]–[24], vision-based flight [25]–[28] and dynamic obstacle avoidance [29]–[32]. However, this platform compared to the other has less stability and more higher noise level due to use to be generally multicopter. Moreover, to achieve fully-actuated systems, quadcopter designers either increase the number of motors or add a servo mechanism to rotate the motor. This arrangement makes quadcopters more complex and high-cost [33], [34]. Robotic hummingbird is used owing to high maneuver capability, confidentiality, low power consumption and biomimetic design [13], [35]–[37]. Nonetheless, this platform is insufficient due to its complex mechanical structure, limited payload capacity, short flight time and wind sensitivity. Coaxial rotor UAVs, particularly helicopters, have gained considerable traction due to their lower noise levels and greater stability. [38]–[41]. However, coaxial helicopters have a swashplate mechanism which generates orientation movements in two-axes (roll&pitch) and a tail which plays a critical role in flight dynamics. Due to these dependencies, coaxial helicopters are more complex and more need a maintenance.

To eliminated those disadvantages was invented the swashplateless mechanism [42]. With this mechanism, a simple structure and less maintenance are achieved. Moreover, the simplicity of this platform is increased payload capacity and reduced system cost [43]. The swashplateless mechanism is used in different applications. Some of the impressive achievements with swashplateless mechanism designed MARs have reached the limits of the existing other platform [44]–[47]. Moreover, it has been more successful in some applications [47]. However, the design criteria for the potential to improve the performance of the swashplateless mechanism have a knowledge gap. This mechanism only studied scalability in different propeller dimensions [48]. The hinged angle in the swashplateless mechanism is one of the most important design parameters. The hinged angle is directly related to control precision, stability, maneuver capability and power consumption [49], [50]. This relationship is particularly important in applications where aerial robots are expected to perform tasks with lower power consumption. However, no study examines the controller performance of different hinge angles in an aerial robot using a swashplateless mechanism. This study aims to address this gap by investigating the effects of different hinge angles on controller performance according to controller metrics and under disturbance effects.

In this study aims to investigate the control performance of different hinge angles for swashplateless MARs. For this reason, this work produced a swashplateless mechanism, the different hinge angles such as $30°, 45°$ and $60°$. The swashplateless mechanism with different hinge angles has been evaluated in 2-DOF test platform. With this test platform is evaluated which designed attitude controller (pitch and roll). The research contributions are as follows:

- The effect of different hinge angles on controller performance is demonstrated in a real-world deployment.
- A test platform with 2-DOF has been developed to investigate controller performance without being in flight.

2. Method

In this section, the working principle of a swashplateless mechanism, 2 degree-of-freedom (DOF) test platform and controller design procedure designed for this mechanism has been informed. The 2-DOF test platform provides controlled investigation, testing and determination of the swashplateless mechanism's response to the orientation commands, presenting perspective to dynamics and control approach under different disturbances. The working principle of the swashplateless mechanism is carefully explained in detail, particularly its effects on the controller performance of the different hinge angles. In addition, the control strategy as a baseline implemented to achieve reference tracking

of the micro aerial robots (MARs) orientation angles is described, and the methodology used to evaluate controller performance on the 2-DOF test platform. The 2-DOF test platform used in experiment tests is shown in Fig. 1.

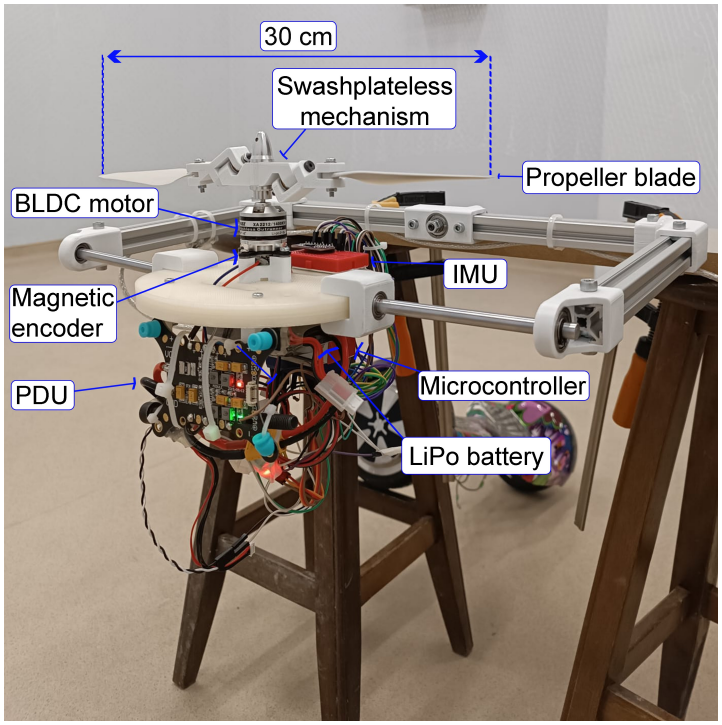

Fig. 1. Demonstration of a swashplateless mechanism with 2-DOF test platform

The 2-DOF test platform is designed to investigate the roll and pitch angle reference tracking performance of the swashplateless mechanism used in MARs [51]. This platform provided a controllable test environment to evaluate the controller performance of MARs to be airborne. This approach presents a perspective that minimizes risk, reduces setup costs and provides different controller observation capabilities with different hinge angles in real-world conditions.

2.1. Design of the 2-DOF Test Platform

With this test platform, the effects of different hinge angles on the swashplateless mechanism are investigated in terms of controller performance. A more general result can be obtained by increasing the degrees of freedom on the test platform to investigate controller performance and different hinge angles. However, in this study, 2-DOF is considered sufficient to show the effect of different hinge angles on controller performance. Both the fittings of the 2-DOF test platform and the swashplateless mechanism are produced of polylactic acid (PLA) material using 3D printing technology. PLA material was preferred for this study owing to its both cost-effective and lightweight characteristic properties and allowing for a capable accurate representation of the MARs dynamics. A 20x20 mm sigma profile joint equipment was also used for the test platform. The preferred propeller for this passive mechanism is 8.46x1 inch and has a total length of 30 cm including swashplateless mechanism. This 2-DOF test platform is capable of both roll and pitch orientation. The diagram of the electronic components used in the 2-DOF test platform is shown in Fig. 2.

The MAR, whose performance was analysed on the 2-DOF test platform, has several electronic components, including power distribution unit (PDU), 11.1V (3S) 1.5Ah LiPo battery, Teensy 4.1 32-bit ARM-based microcontroller with 600 Mhz processing capability, BNO080 6-DOF inertial measurement unit (IMU), Emax XA2212 1400KV brushless direct current (BLDC) motor, AS5600

magnetic encoder, BLHeli electronic speed controller (ESC) 30A and AS5600 magnetic encoder.

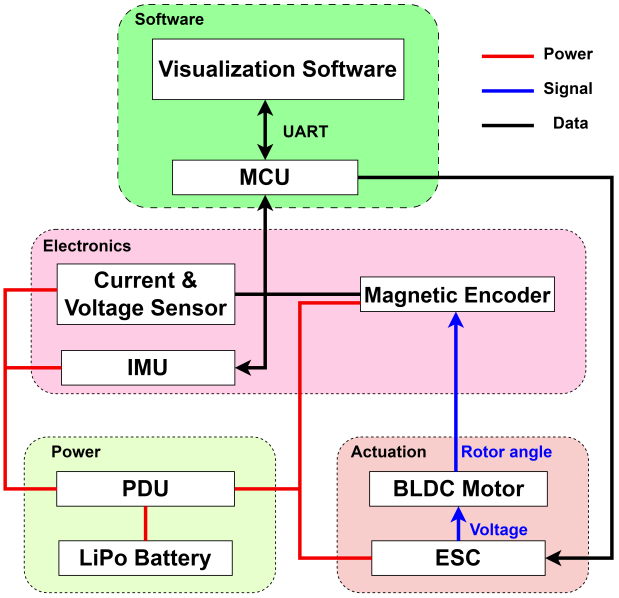

Fig. 2. Demonstration of the electronic component diagram [50]

2.2. Working Principle of the Swashplateless Mechanism

This section has explained the swashplateless mechanism, which uses a single motor to provide both position and orientation movement. Unlike classic multi-actuator setups, this mechanism presents movement through a passive design that includes angled hinges and positive and negative blades, providing for the simplified but alternative design approach to achieving orientation and position. By applying the sinusoidal throttle signal, the passive mechanism generates a differential pitch angle across the positive and negative blades, obtaining a net moment that orientations and positions the MARs. This section further explains on the structural components of the swashplateless mechanism. The swashplateless mechanism used in experiment tests is shown in Fig. 3.

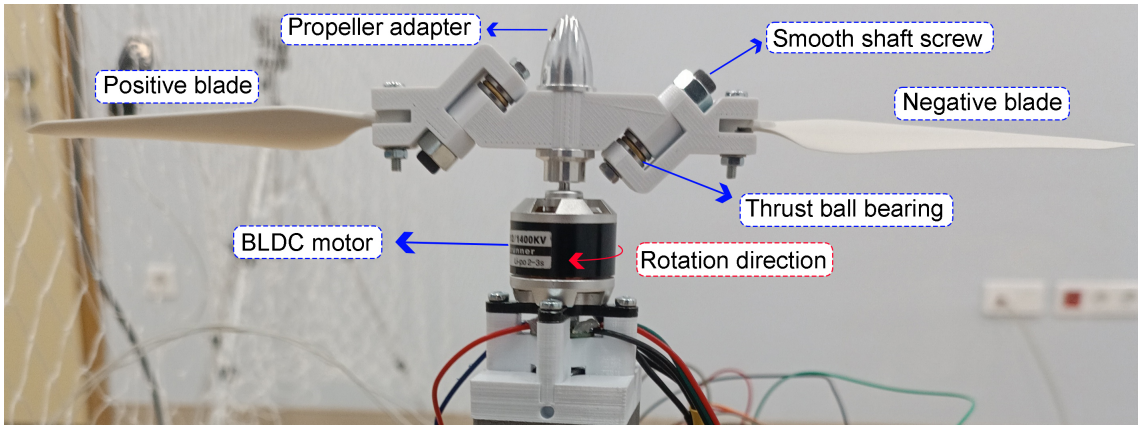

Fig. 3. Mechanical structure of swashplateless mechanism [50]

Unlike the standard propeller, the swashplateless mechanism has a passive mechanism between the propeller blades. This passive mechanism consists of blade holders and the main body part. Swashplateless mechanism and BLDC motor connection are realised through the propeller adapter. The thrust ball bearing between the main body and blade holder is added to reduce friction. This

approach both simplified the control system by reducing the need for additional actuators and reduced power consumption in the MARs [47]. The integration of these passive elements is considered an alternative compact and efficient design solution. The passive mechanism with tilted asymmetric hinges is shown in Fig. 4.

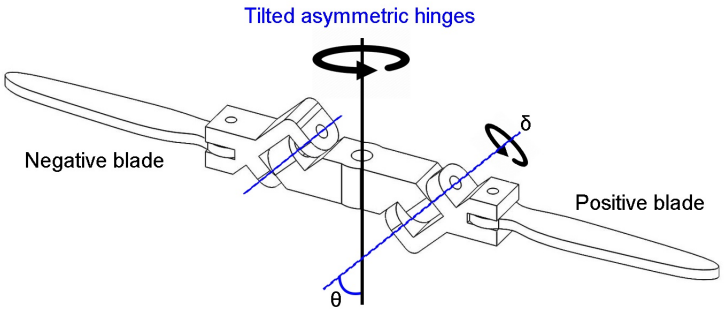

Fig. 4. Passive swashplateless mechanism added between the blades [50]

In this mechanism, a hinge angle (θ) is formed between the main body part and the blade holder. This hinge angle is a critical design parameter that affects stability, vibration and cyclic control. In addition, owing to both hinges angle and blade inertia, a lag angle (δ). In the swashplateless mechanism, the angles formed during the movement of the propeller are presented in Fig. 5.

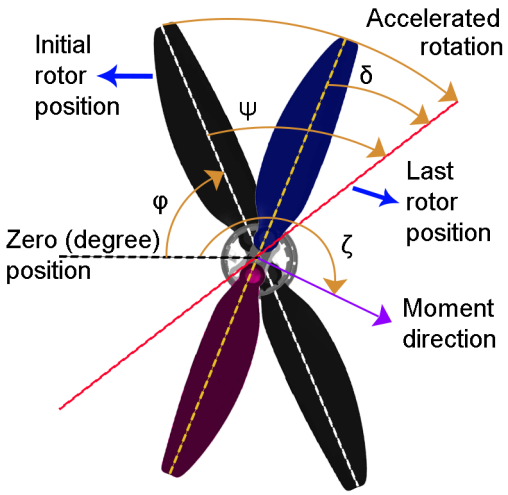

Fig. 5. Examining the angles formed on the propeller [50]

A cyclic throttle signal must be applied to generate an orientation movement with the swashplateless mechanism. For this cyclic signal modulation be measurement actual rotor position. Before the cyclic signal modulation is the initial rotor position angle (ϕ). After the cyclic throttle signal, it is expected that the last rotor position ($\phi + \psi$) will be reached. However, due to the inertia of the propeller, it is not possible to reach this last rotor position. The actual rotor position will therefore be ($\phi + \psi - \delta$). Both the application of a cyclic throttle signal and the tilted asymmetric hinge angle of the swashplateless passive mechanism create different pitch angles between the positive and negative blades. This differential pitch angle results in a net moment across the propeller plane, perpendicular to the actual blade position. This orientation angle of the net moment is called ζ.

The throttle signal applied to the BLDC motor connected to the swashplateless mechanism is related to both altitude and orientation movement. The signal of cyclic throttle S_t, which related both

position and orientation control components,is defined as below:

$$S_t = S_a + S_c cos(\alpha - \phi) \tag{1}$$

Where α is the actual rotor position by the AS5600 magnetic encoder, ϕ is the rotor acceleration position angle, S_c is the cyclic signal value and S_a is the nominal value of the throttle used to reach the desired altitude. The resulting thrust force F_T and torque M_C generated by the swashplateless mechanism are calculated as follows:

$$F_T = k_t S_a, M_C = k_m S_c \tag{2}$$

Where F_T is the thrust force generated from the BLDC motor and M_C represents the magnitude of the moment. Using the data obtained by the swashplateless mechanism, k_t and k_m can be determined in (2). Similarly, it has been shown that this computation can be used in single-actuator unmanned aerial vehicle (UAV) autonomous navigation scenarios with a swashplateless mechanism [47]. The orientation angle of the net moment, ζ, which is generated by the swashplateless mechanism is shown below:

$$\zeta = \phi + \psi - \delta + \pi/2 \tag{3}$$

Where ψ, is the angle between the initial rotor angle and the accelerated rotation, δ is the lag angle in the passive swashplateless mechanism. This angle is formed according to tilted asymmetric hinges and is directly related to the determination orientation angle of the moment.

2.3. Controller Design for the Swashplateless Mechanism

This study investigates the relationship between control performance and different hinge angles. Control performance is evaluated on the 2-DOF test platform without being in flight. Different roll and pitch angle references are applied to investigate the effect on the control performance of different hinge angles in the swashplateless mechanism. The tests provide an example of real-world operating conditions and show how performance criteria such as rise, settling time and ITAE affect different hinge angles. This study aims to investigate to determination between the different hinge angles and controller performance for the MARs. The results will provide for improving design and both development of controller and swashplateless mechanism progress in the future. The controller schema designed for roll and pitch angle reference tracking is shown in Fig. 6.

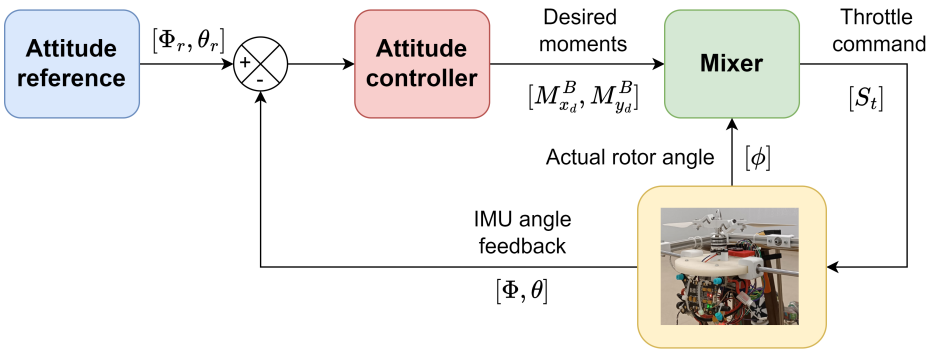

Fig. 6. The controller schema for the reference tracking

In experimental tests, both roll and pitch angles are used as a reference for determining control performance. A Proportional-Integral (PI) algorithm was used as the attitude controller for reference

tracking and tuned experimentally. A PI controller was chosen for its simplicity, effectiveness and easy of tuning. As the experimental setup focused on investigating the effect of different hinge angle on control performance, the PI controller provided the required control without the complexity of a derivative term. The absence of derivative term also reduced the sensitivity of measurement noise from the IMU. In addition, the use of the PI controller contributed to the clarity of the objectives of the research. The output of the PI controller was the desired moments on both the x and y axes. The desired moments are determined as follows:

$$M^B_{xy,d} = K_{xy,p}\Phi_e|\theta_e + K_{xy,i}\int_0^t \Phi_e|\theta_e dt \tag{4}$$

Where $\Phi_e|\theta_e$ is calculated as $\Phi_e = \Phi_r - \Phi$ and $\theta_e = \theta_r - \theta$. K_p and K_i are the proportional and integral coefficients in a PI controller. For the calculated throttle command, which is the output of the Mixer algorithm, S_a and S_c must be specified in (1). These values are calculated as follows:

$$S_a = \frac{F_{T,d}}{k_t}, \quad S_c = \frac{\|M^B_{xy,d}\|}{k_m} \tag{5}$$

Where $F_{T,d}$ is used as the default value because the 2-DOF test platform does not allow z-axis position change. The S_c value can be determined according to the relationship between the controller output ($\|M^B_{xy,d}\|$) and a previously estimated coefficient (k_m). The orientation angle of the moment is determined as below:

$$\zeta = atan2(M^B_{y,d}, M^B_{x,d}) \tag{6}$$

Where after the ζ calculating, ϕ rotor acceleration angle can be determined as $\phi = \zeta - \psi + \delta - \pi/2$. Once these have been calculated, the S_t throttle command sent to ESC can be determined.

3. Experiment Results and Analysis

In this section, the experimental results are presented in such a way as to provide a clear analysis of the control performance of different hinge angles in the swashplateless mechanism under different conditions. The results are organized in three parts: firstly, the swashplateless mechanism's roll and pitch response to reference inputs under normal conditions; secondly, its response to reference inputs under the wind disturbances; and finally, a main findings, comparison of other studies and strengths and limitations.

3.1. The Controller Performance Under Normal Conditions

This section presented a series of real-world experiments. All experiments were performed on the 2-DOF test platform. Firstly, the effects of different hinge angles on the swashplateless mechanism were investigated under normal conditions. The response to a pitch angle reference of 0.1 radians is shown in Fig. 7.

The different hinge angles were preferred as 30°,45° and 60°. According to this pitch angle reference result, the 30° hinge angle was observed to perform the others. The swashplateless mechanism with 60° hinge angle has been detected as not reaching to given 0.1 radians reference pitch angle. The swashplateless mechanism with a 45° hinge angle achieved the reference but it had a higher rise time value. Table 1 summarizes the comparative performance metrics of different hinge angles in the pitch reference tracking.

The swashplateless mechanism with a 30° hinge angle was observed to perform better with less 36.2% rise time, 17.28% settling time and 57.69% integral of the time absolute of error (ITAE) than

the nearest hinge angle. According to this result, less hinge angle is formed and less angular deflection in the propeller blade which generally results in better controller precision. Therefore, The 30° hinge angle reduces angular deflection, resulting in improved controller precision and faster rise times due to perform better energy transfer to the propeller blades. The response to a roll angle reference of 0.1 radians is present in Fig. 8.

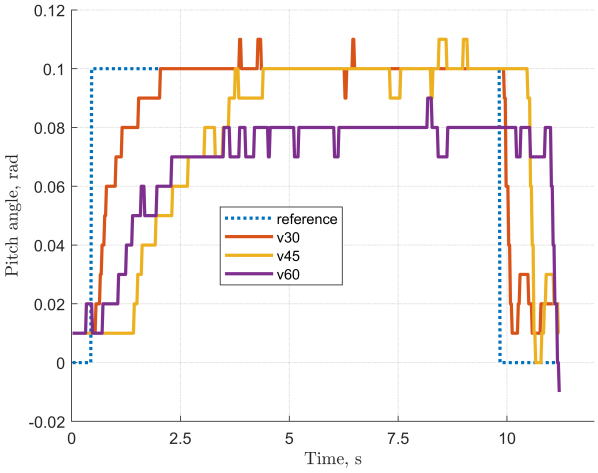

Fig. 7. Response of different hinge angles to pitch angle reference tracking

Table 1. Performance metrics (rise time, overshoot, settling time and ITAE) for the different hinge angles in pitch reference tracking

Hinge angle (degrees)	Rise time (s)	Overshoot (%)	Settling time (s)	Error (ITAE)
30	**1.48**	10	**5.84**	**2.56**
45	2.32	10	7.06	6.05
60	NaN	0	NaN	15.08

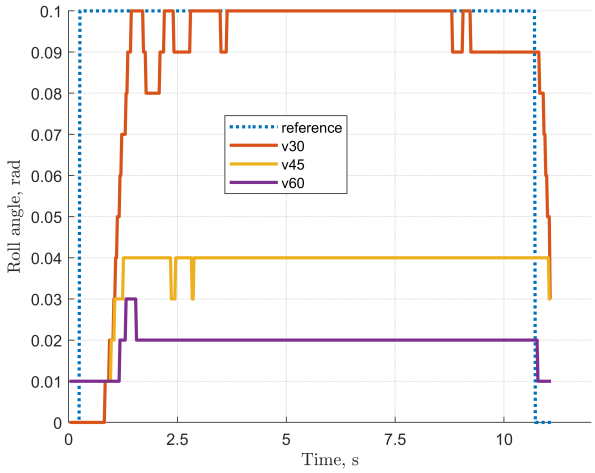

Fig. 8. Response of different hinge angles to roll angle reference tracking

According to this result, the swashplateless mechanisms with a 45° and 60° hinge angle are detected to not reach the given roll reference angle. The 2-DOF test platform shown in Fig. 1 has

a dimension of 26x42 cm. The distance of the BLDC motor centre point is 23 cm from the rotation point in the x-axis on the 2-DOF test platform. In this instance, only the swashplateless mechanism with a hinge angle of 30° is observed to be capable of generating a moment that can reach the roll reference angle. The comparative performance of different hinge angles in the roll reference tracking are shown in Table 2.

Table 2. Performance metrics (rise time, overshoot, settling time and ITAE) for the different hinge angles in roll reference tracking

Hinge angle (degrees)	Rise time (s)	Overshoot (%)	Settling time (s)	Error (ITAE)
30	**0.5**	0	**1.83**	**5.89**
45	NaN	0	NaN	32.59
60	NaN	0	NaN	41.16

The swashplateless mechanism with a 30° hinge angle was observed to perform better with less 81.92% ITAE than the nearest hinge angle. It was detected that the other hinge angles were incapable of generating enough of a moment and that the more accumulated error value was therefore present.

3.2. The Controller Performance Under Wind Disturbance

This subsection analyses the pitch and roll response of the swashplateless mechanism's to reference inputs under the wind disturbance. The effect of different hinge angles on maintaining stability under these conditions and their role in increasing resilience to environmental disturbances were investigated. The test environment used for the wind disturbance test is depicted in Fig. 9.

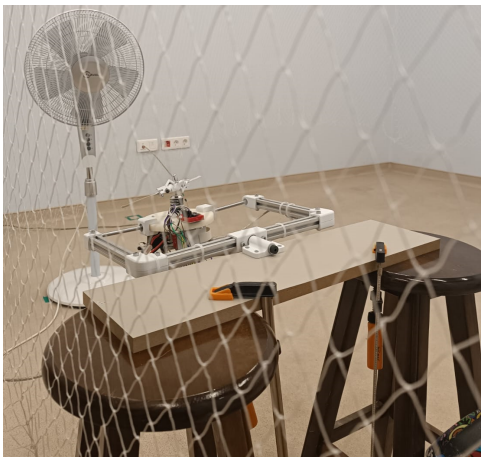

Fig. 9. The wind disturbance test for the different hinge angles

In this environment, the wind generated by the electric fan has an approximate speed of 3.3 m/s. The objective of this test is to assess the disturbance rejection performance of different hinge angles in a swashplateless mechanism. The performance of each hinge angle in tracking the pitch input reference (0.1 radians) under wind disturbance is shown in Fig. 10.

The results of this test indicate that wind disturbance affects all the different hinge angles. The various hinge angles were found to be generally effective in terms of disturbance rejection performance. Table 3 summarizes the comparative performance metrics of different hinge angles when tracking the pitch reference in the presence of wind disturbance.

In this test, the swashplateless mechanism with a hinge angle of 45° was observed to perform better in the presence of wind disturbance in terms of overshoot, settling time, and ITAE criteria. 45° hinge angle was determined to perform better with less 20% overshoot, 16.87% settling time

and 23.36% ITAE than the nearest hinge angle. However, 30° hinge angle was perform better with 91.07% rise time in terms of rise time compared to the nearest hinge angle.

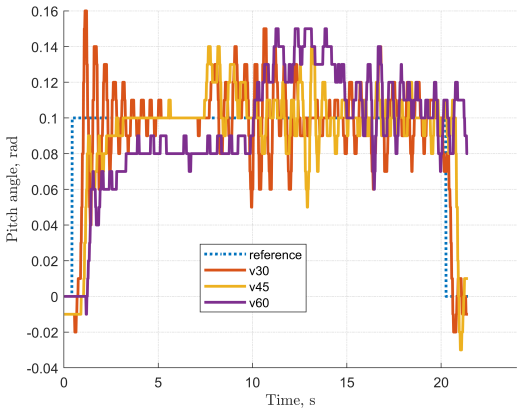

Fig. 10. Response of different hinge angles to pitch angle reference tracking under the wind disturbance

Table 3. Performance metrics (rise time, overshoot, settling time and ITAE) for the different hinge angles when tracking the pitch reference in the presence of wind disturbance

Hinge angle (degrees)	Rise time (s)	Overshoot (%)	Settling time (s)	Error (ITAE)
30	**0.15**	60	NaN	14.3
45	1.68	**40**	**19.81**	**10.96**
60	8.74	50	23.73	24.09

At lower hinge angles, the propeller surfaces generate perpendicular force relative to the MARs body. This results in a reduction of the effective leverage required to control pitch and roll reference. As a consequence, this vertical force affects the damping effect of the passive mechanism. Therefore, a lower hinge angle generally corresponds to a system with lower damping characteristics. However, at high hinge angles (like 60°), the system can damp too much. This over-damping results in slower response and settling times. Due to the above explanations, the 30° hinge angle has a faster response time, but higher overshoot and settling time performance. The performance of each hinge angle in tracking the roll input reference (0.1 radians) under wind disturbance is shown in Fig. 11.

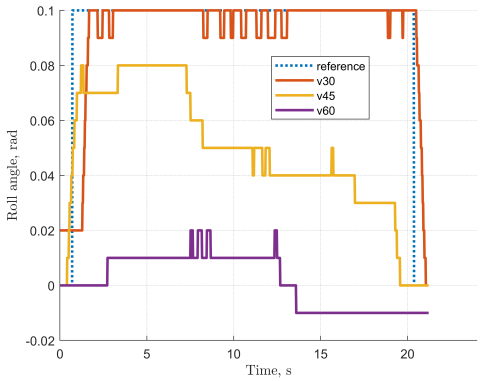

Fig. 11. Response of different hinge angles to roll angle reference tracking under the wind disturbance

Similarly, the results indicate that swashplateless mechanisms with a 45° and 60° hinge angle are unable to reach the specified roll reference angle in the presence of wind disturbance. It was observed that both 45° and 60° hinge angles could not reach the roll reference because they could not produce enough moment. The swashplateless mechanisms with a 30° hinge angle have been observed to resistance show to wind disturbance in the roll angle reference. The comparative performance of different hinge angles when tracking the roll reference in the presence of wind disturbance are shown in Table 4.

Table 4. Performance metrics (rise time, overshoot, settling time and ITAE) for the different hinge angles when tracking the roll reference in the presence of wind disturbance

Hinge angle (degrees)	Rise time (s)	Overshoot (%)	Settling time (s)	Error (ITAE)
30	**0.94**	0	**19.02**	**4.23**
45	NaN	0	NaN	45.65
60	NaN	0	NaN	133.87

The swashplateless mechanism with a 30° hinge angle was observed to perform better with less %90.73 ITAE than the nearest hinge angle under the wind disturbance. The efficacy of hinge angles in resisting wind disturbance and tracking references has been shown through a series of experimental tests.

3.3. Discussion

This study was discussed and evaluated in terms of main findings, comparison of other studies, implications and explanation of findings and strengths and limitations.

Main findings: According to the experimental results, this study shows that a 30° hinge angle gives the best overall performance in terms of rise time, overshoot, settling time, ITAE and disturbance rejection compared to 45° and 60° hinge angles. This evaluation was performed according to the pitch and roll angle control. This study demonstrated the effect on controller performance of hinge angle for the swashplateless mechanism.

Comparison of other studies: when compared the other studies, such as [49], the variation of the hinge angle affects the lag angle formation, which in turn affects the differential pitch angle between different propeller blades. Previous studies have shown that less hinge angle allows more lag angle to be formed. This study has shown that more lag angle can be defined as an aspect that improves control performance.

Implications and explanation of findings: the results suggest that the smaller hinge angle increases the lag angle and improves the controller performance by robustness to disturbances. This finding is particularly important for the design of aerial robots, which are expected to demonstrate robust performance in unpredictable environments. Smaller hinge angles, such as 30°, not only improve performance but also contribute to disturbance rejection in the swashplateless mechanism.

Strengths and limitations: one of the strengths of this study is that a comprehensive experimental approach is adopted to evaluate the effect of different hinge angles on both controller performance and wind disturbance. However, a limitation of this study is that only pitch and roll angles can be tested on the 2-DOF platform. This test platform is not suitable for generating both orientation and position changes. The development of a test platform with multi-DOF could be the focus of future work.

4. Conclusions

This study investigated the effect of different hinge angles in the swashplateless mechanism in terms of control performance. The design, working principle and controller schema are presented

in the swashplateless mechanism. The efficacy of both reference tracking and disturbance rejection performance has been demonstrated in a variety of scenarios on the 2-DOF test platform without being in flight. These results demonstrated that a 30° hinge angle best overall performance according to the reference tracking and wind disturbance compared to the others, as well as the effect on controller performance of hinge angle for the swashplateless mechanism. This study contributes to the growing knowledge of the swashplateless mechanism used in MARs by investigating the relationship between controller performance and different hinge angles. These findings indicate that the hinge angle should be preferred based on the performance requirements in real-world scenarios. In the future, the goal will be to improve flight performance both by implementing more sophisticated controllers such as model predictive control (MPC) and robust control in addition to proportional-integral-derivative (PID) and by extending this work to multi-DOF platforms and testing different wind and load conditions.

Author Contribution: The author is the sole contributor to this work and has approved the final manuscript.

Funding: This research received no external funding.

Conflicts of Interest: The author declare no conflict of interest.

References

[1] A. Suarez, R. Salmoral, A. Garofano-Soldado, G. Heredia and A. Ollero, "Aerial Device Delivery for Power Line Inspection and Maintenance," *2022 International Conference on Unmanned Aircraft Systems (ICUAS)*, pp. 30-38, 2022, https://doi.org/10.1109/ICUAS54217.2022.9836039.

[2] G. Li, R. Ge, and G. Loianno, "Cooperative transportation of cable suspended payloads with mavs using monocular vision and inertial sensing," *IEEE Robotics and Automation Letters*, vol. 6, no. 3, pp. 5316–5323, 2021. https://doi.org/10.1109/LRA.2021.3065286

[3] L. Qian and H. H. T. Liu, "Path-Following Control of A Quadrotor UAV With A Cable-Suspended Payload Under Wind Disturbances," in *IEEE Transactions on Industrial Electronics*, vol. 67, no. 3, pp. 2021-2029, 2020, 10.1109/TIE.2019.2905811.

[4] F. Hauf *et al*., "Learning Tethered Perching for Aerial Robots," *2023 IEEE International Conference on Robotics and Automation (ICRA)*, pp. 1298-1304, 2023, https://doi.org/10.1109/ICRA48891.2023.10161135.

[5] N. Imanberdiyev, S. Sood, D. Kircali, and E. Kayacan, "Design, development and experimental validation of a lightweight dual-arm aerial manipulator with a cog balancing mechanism," *Mechatronics*, vol. 82, p. 102719, 2022. https://doi.org/10.1016/j.mechatronics.2021.102719.

[6] F. Paredes-Vallés, J. J. Hagenaars, J. Dupeyroux, S. Stroobants, Y. Xu, and G. de Croon, "Fully neuromorphic vision and control for autonomous drone flight," *Science Robotics*, vol. 9, no. 90, 2024. https://doi.org/10.1126/scirobotics.adi0591.

[7] V. Wüest, S. Jeger, M. Feroskhan, E. Ajanic, F. Bergonti, and D. Floreano, "Agile perching maneuvers in birds and morphing-wing drones," *Nature Communications*, vol. 15, no. 1, p. 8330, 2024. https://doi.org/10.1038/s41467-024-52369-4.

[8] K. Takaya, H. Ohta, V. Kroumov, K. Shibayama and M. Nakamura, "Development of UAV System for Autonomous Power Line Inspection," *2019 23rd International Conference on System Theory, Control and Computing (ICSTCC)*, pp. 762-767, 2019, https://doi.org/10.1109/ICSTCC.2019.8885596.

[9] A. Hegde and D. Ghose, "Multi-uav collaborative transportation of payloads with obstacle avoidance," *IEEE Control Systems Letters*, vol. 6, pp. 926–931, 2021, https://doi.org/10.1109/LCSYS.2021.3087339.

[10] A. T. Karaşahin, "Genetically tuned linear quadratic regulator for trajectory tracking of a quadrotor," *Academic Platform Journal of Engineering and Smart Systems*, vol. 12, no. 1, pp. 37–46, 2024, https://doi.org/10.21541/apjess.1316025.

[11] D. Falanga, K. Kleber, S. Mintchev, D. Floreano, and D. Scaramuzza, "The foldable drone: A morphing quadrotor that can squeeze and fly," *IEEE Robotics and Automation Letters*, vol. 4, pp. 209–216, 2019, https://doi.org/10.1109/LRA.2018.2885575.

[12] V. Kumar and N. Michael, "Opportunities and challenges with autonomous micro aerial vehicles," *The International Journal of Robotics Research*, vol. 31, no. 11, pp. 1279–1291, 2012, https://doi.org/10.1007/978-3-319-29363-9_3.

[13] J. Zhang, F. Fei, Z. Tu, and X. Deng, "Design optimization and system integration of robotic hummingbird," *Proceedings - IEEE International Conference on Robotics and Automation*, pp. 5422–5428, 2017, https://doi.org/10.1109/ICRA.2017.7989639.

[14] D. Coleman, M. Benedict, V. Hrishikeshavan, and I. Chopra, "Design, development and flight-testing of a robotic hummingbird," in *AHS 71st annual forum*, pp. 5–7, 2015, https://doi.org/10.4050/F-0071-2015-10503.

[15] S. George and P. Samuel, "On the design and development of a coaxial nano rotorcraft," *50th AIAA Aerospace Sciences Meeting Including the New Horizons Forum and Aerospace Exposition*, 2012, https://doi.org/10.2514/6.2012-585.

[16] M. Brunner, K. Bodie, M. Kamel, M. Pantic, W. Zhang, J. Nieto, and R. Siegwart, "Trajectory tracking nonlinear model predictive control for an overactuated mav," *Proceedings - IEEE International Conference on Robotics and Automation*, pp. 5342–5348, 2020, https://doi.org/10.1109/ICRA40945.2020.9197005.

[17] Y. Song, A. Romero, M. Müller, V. Koltun, and D. Scaramuzza, "Reaching the limit in autonomous racing: Optimal control versus reinforcement learning," *Science Robotics*, vol. 8, no. 82, 2023, https://doi.org/10.1126/scirobotics.adg1462.

[18] M. O'Connell, G. Shi, X. Shi, K. Azizzadenesheli, A. Anandkumar, Y. Yue, and S.-J. Chung, "Neural-fly enables rapid learning for agile flight in strong winds," *Science Robotics*, vol. 7, no. 66, 2022, https://doi.org/10.1126/scirobotics.abm6597.

[19] S. Sun, A. Romero, P. Foehn, E. Kaufmann, and D. Scaramuzza, "A comparative study of nonlinear mpc and differential-flatness-based control for quadrotor agile flight," *IEEE Transactions on Robotics*, vol. 38, no. 6, pp. 3357–3373, 2022, https://doi.org/10.1109/TRO.2022.3177279.

[20] Y. Song and D. Scaramuzza, "Policy search for model predictive control with application to agile drone flight," *IEEE Transactions on Robotics*, vol. 38, no. 4, pp. 2114–2130, 2022, https://doi.org/10.1109/TRO.2022.3141602.

[21] A. Loquercio, E. Kaufmann, R. Ranftl, M. Müller, V. Koltun, and D. Scaramuzza, "Learning high-speed flight in the wild," *Science Robotics*, vol. 6, no. 59, 2021, https://doi.org/10.1126/scirobotics.abg5810.

[22] A. Saviolo and G. Loianno, "Learning quadrotor dynamics for precise, safe, and agile flight control," *Annual Reviews in Control*, vol. 55, pp. 45–60, 2023, https://doi.org/10.1016/j.arcontrol.2023.03.009.

[23] A. Loquercio, A. Saviolo, and D. Scaramuzza, "Autotune: Controller tuning for high-speed flight," *IEEE Robotics and Automation Letters*, vol. 7, no. 2, pp. 4432–4439, 2022, https://doi.org/10.1109/LRA.2022.3146897.

[24] P. Foehn, D. Brescianini, E. Kaufmann, T. Cieslewski, M. Gehrig, M. Muglikar, and D. Scaramuzza, "Alphapilot: Autonomous drone racing," *Autonomous Robots*, vol. 46, no. 1, pp. 307–320, 2022, https://doi.org/10.1007/s10514-021-10011-y.

[25] P. Foehn, E. Kaufmann, A. Romero, R. Penicka, S. Sun, L. Bauersfeld, T. Laengle, G. Cioffi, Y. Song, A. Loquercio *et al.*, "Agilicious: Open-source and open-hardware agile quadrotor for vision-based flight," *Science robotics*, vol. 7, no. 67, 2022, https://doi.org/10.1126/scirobotics.abl6259.

[26] A. Beyeler, J.-C. Zufferey, and D. Floreano, "Vision-based control of near-obstacle flight," *Autonomous robots*, vol. 27, no. 3, pp. 201–219, 2009, https://doi.org/10.1007/s10514-009-9139-6.

[27] J. Xing, L. Bauersfeld, Y. Song, C. Xing and D. Scaramuzza, "Contrastive Learning for Enhancing Robust Scene Transfer in Vision-based Agile Flight," *2024 IEEE International Conference on Robotics and Automation (ICRA)*, pp. 5330-5337, 2024, https://doi.org/10.1109/ICRA57147.2024.10610095.

[28] J. Lin, Y. Wang, Z. Miao, H. Zhong, and R. Fierro, "Low-complexity control for vision-based landing of quadrotor uav on unknown moving platform," *IEEE Transactions on Industrial Informatics*, vol. 18, no. 8, pp. 5348–5358, 2021, https://doi.org/10.1109/TII.2021.3129486.

[29] D. Falanga, K. Kleber, and D. Scaramuzza, "Dynamic obstacle avoidance for quadrotors with event cameras," *Science Robotics*, vol. 5, no. 40, 2020, https://doi.org/10.1126/scirobotics.aaz9712.

[30] B. Lindqvist, S. S. Mansouri, A.-a. Agha-mohammadi, and G. Nikolakopoulos, "Nonlinear mpc for collision avoidance and control of uavs with dynamic obstacles," *IEEE robotics and automation letters*, vol. 5, no. 4, pp. 6001–6008, 2020, https://doi.org/10.1109/LRA.2020.3010730.

[31] J. Qi, J. Guo, M. Wang, C. Wu, and Z. Ma, "Formation tracking and obstacle avoidance for multiple quadrotors with static and dynamic obstacles," *IEEE Robotics and Automation Letters*, vol. 7, no. 2, pp. 1713–1720, 2022, https://doi.org/10.1109/LRA.2022.3140830.

[32] B. Wang, Y. Zhang, and W. Zhang, "Integrated path planning and trajectory tracking control for quadrotor uavs with obstacle avoidance in the presence of environmental and systematic uncertainties: Theory and experiment," *Aerospace Science and Technology*, vol. 120, p. 107277, 2022, https://doi.org/10.1016/j.ast.2021.107277.

[33] P. Zheng, X. Tan, B. B. Kocer, E. Yang, and M. Kovac, "Tiltdrone: A fully-actuated tilting quadrotor platform," *IEEE Robotics and Automation Letters*, vol. 5, pp. 6845–6852, 2020, https://doi.org/10.1109/LRA.2020.3010460.

[34] M. Ryll, H. H. Bülthoff, and P. R. Giordano, "A novel overactuated quadrotor unmanned aerial vehicle: Modeling, control, and experimental validation," *IEEE Transactions on Control Systems Technology*, vol. 23, no. 2, pp. 540–556, 2014, https://doi.org/10.1109/TCST.2014.2330999.

[35] M. Keennon, K. Klingebiel, and H. Won, "Development of the nano hummingbird: A tailless flapping wing micro air vehicle," in *50th AIAA aerospace sciences meeting including the new horizons forum and aerospace exposition*, p. 588, 2012, https://doi.org/10.2514/6.2012-588.

[36] J. Zhang, Z. Tu, F. Fei and X. Deng, "Geometric flight control of a hovering robotic hummingbird," *2017 IEEE International Conference on Robotics and Automation (ICRA)*, pp. 5415-5421, 2017, https://doi.org/10.1109/ICRA.2017.7989638.

[37] Z. Tu, F. Fei, J. Zhang, and X. Deng, "An at-scale tailless flapping-wing hummingbird robot. i. design, optimization, and experimental validation," *IEEE Transactions on Robotics*, vol. 36, no. 5, pp. 1511–1525, 2020, https://doi.org/10.1109/TRO.2020.2993217.

[38] A. Koehl, H. Rafaralahy, M. Boutayeb, and B. Martinez, "Aerodynamic modelling and experimental identification of a coaxial-rotor uav," *Journal of Intelligent & Robotic Systems*, vol. 68, pp. 53–68, 2012, https://doi.org/10.1007/s10846-012-9665-x.

[39] Z.-Y. Lv, Y. Wu, Q. Zhao, and X.-M. Sun, "Design and control of a novel coaxial tilt-rotor uav," *IEEE Transactions on Industrial Electronics*, vol. 69, no. 4, pp. 3810–3821, 2021, https://doi.org/10.1007/s10514-009-9139-6.

[40] Z. Lv, Y. Sun, S. Li, Y. Wu, and X.-M. Sun, "Coaxial tilt-rotor uav: Fixed-time control, mixer, and flight test," *IEEE Transactions on Intelligent Vehicles*, 2024, https://doi.org/10.1109/TIV.2024.3453208.

[41] L. Chen, J. Xiao, Y. Zheng, N. A. Alagappan, and M. Feroskhan, "Design, modeling, and control of a coaxial drone," *IEEE Transactions on Robotics*, 2024, https://doi.org/10.1109/TRO.2024.3354161.

[42] J. Paulos and M. Yim, "An underactuated propeller for attitude control in micro air vehicles," *IEEE International Conference on Intelligent Robots and Systems*, pp. 1374–1379, 2013, https://doi.org/10.1109/IROS.2013.6696528.

[43] M. Yim and J. Paulos, "Flight performance of a swashplateless micro air vehicle," *Proceedings - IEEE International Conference on Robotics and Automation*, vol. 2015, pp. 5284–5289, 2015, https://doi.org/10.1109/ICRA.2015.7139936.

[44] Y. Qin, N. Chen, Y. Cai, W. Xu, and F. Zhang, "Gemini ii: Design, modeling, and control of a compact yet efficient servoless bi-copter," *IEEE/ASME Transactions on Mechatronics*, vol. 27, pp. 4304–4315, 2022, https://doi.org/10.1109/TMECH.2022.3153587.

[45] H. Li, N. Chen, F. Kong, Y. Zou, S. Zhou, D. He, and F. Zhang, "Halo: A safe, coaxial, and dual-ducted uav without servo," *2023 IEEE/RSJ International Conference on Intelligent Robots and Systems (IROS)*, pp. 6935–6941, 2023, https://doi.org/10.1109/IROS55552.2023.10341923.

[46] N. Chen, F. Kong, H. Li, J. Liu, Z. Ye, W. Xu, F. Zhu, X. Lyu, and F. Zhang, "Swashplateless-elevon actuation for a dual-rotor tail-sitter vtol uav," *2023 IEEE/RSJ International Conference on Intelligent Robots and Systems (IROS)*, pp. 6970–6976, 2023, https://doi.org/10.1109/IROS55552.2023.10341861.

[47] N. Chen, F. Kong, W. Xu, Y. Cai, H. Li, D. He, Y. Qin, and F. Zhang, "A self-rotating, single-actuated uav with extended sensor field of view for autonomous navigation," *Science Robotics*, vol. 8, 2023, https://doi.org/10.1126/scirobotics.ade4538.

[48] J. J. Paulos and M. Yim, "Scalability of cyclic control without blade pitch actuators," in *2018 AIAA Atmospheric Flight Mechanics Conference*, 2018, https://doi.org/10.2514/6.2018-0532.

[49] L. Tang, M. Chang, Y. Huang, S. Zu, and J. Bai, "Parameter effect on the novel swashplateless rotor control," *International Journal of Micro Air Vehicles*, vol. 16, 2024, https://doi.org/10.1177/17568293241238019.

[50] A. T. Karasahin, "Characterization of different hinge angles for swashplateless micro aerial robots," *Engineering Science and Technology, an International Journal*, vol. 55, p. 101750, 2024, https://doi.org/10.1016/j.jestch.2024.101750.

[51] E. B. Jacobsen, *Modelling and control of thrust vectoring mono-copter*, Doctoral dissertation, 2021, https://vbn.aau.dk/ws/files/421577367/Master_Thesis_Emil_Jacobsen_v5.pdf.